Author Manuscript

Author Manuscript

Author Manuscript

Author Manuscript

HHS Public Access

Author manuscript

Reprod Toxicol. Author manuscript; available in PMC 2022 April 01.

Published in final edited form as:

Reprod Toxicol. 2021 April ; 101: 81–92. doi:10.1016/j.reprotox.2021.03.001.

Spatiotemporal evaluation of the mouse embryonic redox environment and histiotrophic nutrition following treatment with valproic acid and 1,2-dithiole-3-thione during early organogenesis

Samantha Lapehn[a,*], **Ted B. Piorczynski**[b], **Jason M. Hansen**[b], **Craig Harris**[a]

[a:] Department of Environmental Health Sciences, University of Michigan, Ann Arbor, MI 48109

[b:] Department of Physiology and Developmental Biology, Brigham Young University, Provo, UT 84602

Abstract

Redox regulation during metazoan development ensures that coordinated metabolic reprogramming and developmental signaling are orchestrated with high fidelity in the hypoxic embryonic environment. Valproic acid (VPA), an anti-seizure medication, is known to increase markers of oxidation and also increase the risk of neural tube defects (NTDs) when taken during pregnancy. It is unknown, however, whether oxidation plays a direct role in failed neural tube closure (NTC). Spatial and temporal fluctuations in total glutathione (GSH) and total cysteine (Cys) redox steady states were seen during a 24hr period of CD-1 mouse organogenesis in untreated conceptuses and following exposure to VPA and the Nrf2 antioxidant pathway inducer, 1,2-dithiole-3-thione (D3T). Glutathione, glutathione disulfide (GSSG), and Cys, cystine (CySS) concentrations, measured in conceptal tissues (embryo/visceral yolk sac) and fluids (yolk sac fluid/amniotic fluid) showed that VPA did not cause extensive and prolonged oxidation during the period of NTC, but instead produced transient periods of oxidation, as assessed by GSH:GSSG redox potentials, which revealed oxidation in all four conceptal compartments at 4, 10, and 14 hours, corresponding to the period of heartbeat activation and NTC. Other changes were tissue and time specific. VPA treatment also reduced total FITC-Ab clearance from the medium over 3hrs, indicating potential disruption of nutritive amino acid supply. Overall, these results indicated that VPA's ability to affect cellular redox status may be limited to tissue-specific windows of sensitivity during the period of NTC. The safety evaluation of drugs used during pregnancy should consider time and tissue specific redox factors.

[*]**Corresponding Author:** Present Address: 1900 9th Ave., Jack R Mac Donald Building, Seattle, WA 98101, slapehn@umich.edu, 330-351-2622.

Declaration of interests

The authors declare that they have no known competing financial interests or personal relationships that could have appeared to influence the work reported in this paper.

Publisher's Disclaimer: This is a PDF file of an unedited manuscript that has been accepted for publication. As a service to our customers we are providing this early version of the manuscript. The manuscript will undergo copyediting, typesetting, and review of the resulting proof before it is published in its final form. Please note that during the production process errors may be discovered which could affect the content, and all legal disclaimers that apply to the journal pertain.

Author Manuscript Author Manuscript Author Manuscript Author Manuscript

Keywords

Redox; Valproic Acid; Organogenesis; Glutathione; Neural Tube Defect; Histiotrophic Nutrition

1. Introduction

The *redox theory of development* describes the strict maintenance of developmental oxygen concentrations required for the regulation of proper redox signaling and control of morphological growth and development (Hansen et al., 2020). Redox signaling is impacted by changes in the concentration of cellular glutathione (GSH), its oxidation state, and other antioxidant levels as well as the direct post-translational modification of protein cysteine (Cys) residues that can affect protein form, abundance, and function (Hansen et al., 2020). Changes to the GSH and glutathione disulfide (GSSG) redox potential (E_h), a measure of cell and tissue-level oxidation, have been shown to correlate with the cellular activities of proliferation, differentiation, apoptosis and necrosis, indicating that redox fluxes in early development have the capacity to act as signaling mechanisms for developmental stage progression (Schafer & Buettner, 2001). The organogenesis stage of development occurs under conditions of hypoxia where oxygen concentrations (O_2) range between 7–18mmHg and encompass the period during which the developing embryo is most susceptible to morphological birth defects, such as those relating to neural tube closure, limb abnormalities and heart defects (Greene & Copp, 2014; Hansen et al., 2020). Many teratogenic compounds associated with structural birth defects have previously been implicated in redox manipulation during development supporting the potential for oxidizing compounds to disrupt the redox balance required for proper morphogenesis (Hansen, 2006).

This study describes the redox response to VPA, a commonly prescribed anti-epileptic drug that when taken during pregnancy, can lead to an increased risk of the infant developing a neural tube defect (NTD) (Vajda et al., 2013). NTDs are a group of morphological birth defects that result from incomplete neural tube closure (NTC) during early embryonic development that range in severity depending on the timing and location of the failed closure (Greene & Copp, 2014). Risk factors for NTD occurrence have been identified to include genetic mutations, gestational exposure to anti-epileptic and other drugs, and a maternal diet deficient in folic acid during pregnancy, among others (Bruckner et al., 1983; De Marco et al., 2011; Grosse et al., 2016). Despite this evidence, the mechanism of action for spontaneous or VPA-induced NTDs remains unknown, although there is significant evidence from cell, animal, and human studies that VPA exposure causes increases in oxidation markers and is associated with oxidative endpoints (Ahangar et al., 2017; Chaudhary et al., 2015; Komulainen et al., 2015; Palsamy et al., 2014; Tung & Winn, 2011).

Therapeutic and environmental chemicals with pro-oxidant properties have also been implicated in reduced nutrient uptake during organogenesis, where amino acid starvation has been shown to be associated with increased cellular oxidation (Harris et al., 2015; Jilek et al., 2015; Sant et al., 2016a). Prior to the development of a functioning placenta, rodent and human embryonic nutrition rely on nutrient uptake via a process of histiotrophic nutrition which involves the uptake of proteins and nutrients by the visceral yolk sac (VYS) through

Author Manuscript Author Manuscript Author Manuscript Author Manuscript

receptor mediated endocytosis, followed by proteolysis and utilization of liberated amino acids for protein synthesis (Burton et al., 2002). In addition to serving as a nutritional pathway preceding placental development, histiotrophic nutrition helps to maintain the necessary hypoxic environment during organogenesis by eliminating the need for direct contact with maternal blood and high rates of oxygen delivery (Burton et al., 2001). Decreases in histiotrophic nutrition during organogenesis could promote delayed growth or morphological abnormalities, as well as changes in redox status since histiotrophic nutrition supplies the amino acids needed for synthesis of GSH and other antioxidant compounds (Jilek et al., 2015; Sant et al., 2016a). It is unknown whether VPA acts as an inhibitor of histiotrophic nutrition or whether oxidation may play a role in the decreased histiotrophic uptake seen with other pro-oxidant developmental toxins (Jilek et al., 2015; Sant et al., 2016a).

Due to the rapidly changing and dynamic continuum of developmental events, it is important to understand the spatiotemporal fluctuations in cellular redox states under normal developmental conditions during organogenesis in order to contrast them with the redox profile following perturbations with pro-oxidant agent and commonly prescribed medication, VPA, and the antioxidant response-inducing compound, 1,2-dithiole-3-thione (D3T). D3T is a synthetic chemotherapeutic agent and known inducer of the Nrf2 antioxidant response that has previously been demonstrated to act as an anti-teratogenic compound through reduction of ethanol-induced reactive oxygen species (ROS) generation and apoptosis in pre-treated mouse embryos (Dong et al., 2008; Harris & Hansen, 2012b). Nrf2 is an oxidation responsive transcription factor that under conditions of elevated oxidation translocates to the nucleus where it binds to the antioxidant response element (ARE) and induces the transcription of genes that play a role in glutathione (GSH), thioredoxin, and NADPH regulation (Tonelli et al., 2018). Although VPA exposure has been associated with oxidation endpoints, it suppresses the Nrf2 antioxidant response which could lead to greater oxidative damage (Palsamy et al., 2014). We hypothesized that pre-treatment of mouse embryos with D3T would increase GSH concentrations and elicit a more negative, protective, GSH/GSSG redox potential (E_h) across the time period of neural tube closure from gestational days (GD) 8–9. To assess this, a 24-hour time course of VPA and D3T exposure was performed in organogenesis-stage mouse conceptuses measured in 4 conceptal tissues and fluid compartments including the embryo proper (EMB), visceral yolk sac (VYS), yolk sac fluid (YSF), and amniotic fluid (AF). A histiotrophic nutrition assay was also performed at 1 and 3 hours after D3T, VPA or VPA+D3T exposure to determine whether potential decreases in histiotrophic nutrient uptake may correlate with changes to spatial or temporal redox status. Evaluating redox and nutritional dynamics across developmental time and space will help to generate a map of spatiotemporal redox dynamics during organogenesis under normal and VPA-challenged conditions that will help to identify periods of embryonic oxidant-sensitivity and illuminate a mechanism for VPA induced teratogenesis.

Author Manuscript Author Manuscript Author Manuscript Author Manuscript

2. Materials and Methods

2.1 Animals

Experiments were conducted using mouse whole embryo culture (mWEC) to culture conceptuses from gestational days (GD) 8–9 in time-mated, pregnant CD-1 mice (Charles River Laboratories, Raleigh, NC). The morning following mating with discovery of a vaginal plug was designated as gestational day 0 (GD 0). Animals were housed in groups of 6 or fewer in ventilated cages prior to explant and allowed access to feed and water *ad libitum*. All animal protocols were approved by the University of Michigan Institutional Animal Care and Use Committee and followed the NIH Guide for the Care and Use of Laboratory Animals.

2.2 Culture Conditions

Pregnant GD 8 dams were euthanized by CO_2 asphyxiation and uteri were removed and placed in Tyrode's solution (pH 7.4; HiMedia; Mumbai, India). Intact conceptuses were dissected free from decidual implantation sites with watchmaker's forceps and iridectomy scissors. Maternal tissues including the parietal yolk sac and Reichert's membrane were removed to complete preparation of the conceptus for culture. Conceptuses were cultured in groups of 2–6 per bottle of 2mL of immediately centrifuged female rat serum with 4.3μl/mL penicillin, streptomycin (10,000 units penicillin and 10mg streptomycin per mL, Sigma Aldrich; St. Louis, MO). All culture conditions were at 37°C with gas concentrations at 5% O_2, 5% CO_2, 90% N_2 for 6hrs then 20% O_2, 5% CO_2, 75% N_2 for the remainder of the culture period (Harris, 2012).

2.3 Time Course Exposures and Sampling for Redox HPLC

Pre-treatment of D3T (10μM, <0.01% DMSO v/v, Santa Cruz Biotechnology; Dallas, TX) was administered *in vitro* directly in the female rat serum at the start of the culture period. After two hours, VPA (600μM in H_2O, Sigma-Aldrich; St. Louis, MO) was added *in vitro* to the female rat serum for the VPA and VPA+D3T groups. Samples were collected every 2 hours following the administration of D3T up to 26 hours. Conceptuses were rinsed twice in Hank's Balanced Salt Solution (HBSS, pH 7.4; Thermo Fisher Scientific; Waltham, MA) then pipetted in groups of 2–3 into a 150 μL drop of HBSS in a petri dish where the visceral yolk sac (VYS) was torn and agitated, releasing yolk sac fluid (YSF). The drop of HBSS and YSF was added to a microcentrifuge tube containing 2x HPLC Buffer [10% perchloric acid v/v, 0.4M boric acid, and 20μM γ-glutamylglutamate (γ-EE)]. A second 150 μL drop of HBSS was pipetted over the VYS and embryo (EMB) in the petri dish which were then separated to release amniotic fluid into the HBSS. EMB and VYS were added to separate tubes containing 1x HPLC Buffer and amniotic fluid (AF) was added to a tube with 2x HPLC buffer. All samples were snap frozen in liquid nitrogen and stored at −80°C prior to sample processing. Positive control samples were dosed with mono-ethyl hexyl phthalate (MEHP 100 and 250μg/mL in DMSO <0.1% v/v, Sigma-Aldrich; St. Louis, MO) or tertbutyl hydroquinone (TBHQ 50 and 100 μM, DMSO <0.1% v/v, Sigma-Aldrich; St. Louis, MO) 2 hours following the start of culture and were processed as described above.

Author Manuscript Author Manuscript Author Manuscript Author Manuscript

2.4 Sample preparation and reverse-phase HPLC

EMB, VYS, YSF, and AF samples were sonicated to homogenize tissues then derivatized following the protocol outlined by Jones (Jones, 2002) and modified by Harris and Hansen (Harris & Hansen, 2012a). The bicinchoninic acid (BCA) assay using bovine serum albumin as a standard was performed to determine protein content of samples.

GSH, GSSG, Cys and cystine (CySS) concentrations were determined through reverse-phase HPLC analysis using a Waters 2695 Alliance Separations Module (Milford, MA) fitted with a Supelcosil LC-NH_2 column (Sigma-Aldrich; St. Louis, MO). Mobile phase A consisted of 80% methanol (v/v) and 20% ddiH_2O (v/v) and mobile phase B consisted of 62.5% methanol (v/v), 12.5% glacial acetic acid (v/v), and 214mg/ml sodium acetate trihydrate in ddiH_2O. Samples were run at a gradient flow rate of 1ml/min. Detection of peaks was determined using a Waters 2474 fluorescence detector (excitation 335nm and emission at 518nm) with data analysis on Empower 3 software (Waters; Milford, MA).

2.5 Redox potential, soluble and bound thiol concentration calculations

The Nernst equation was used to calculate the redox potential from concentrations of soluble, GSH, GSSG and Cys, CySS (Harris & Hansen, 2012a; Jones, 2002). VYS and EMB calculations utilized BCA protein concentration data for normalization and YSF and AF samples utilized fluid compartment volume estimations. Fluid compartments volumes were estimated utilizing conceptus images and calculating the volume of spheres ($4\pi r^3$) and subtracting nested compartments. Fluid compartment volumes for 0–12hrs and 14–24hrs were 3μL and 5.9μL for YSF and 1.1μL and 2.4μL for AF. Total Glutathione and total cysteine were calculated as the sum of reduced thiol partner and two times the oxidized thiol partner (GSH + 2GSSG and Cys + 2CySS).

2.6 Histiotrophic Nutrition

Conceptuses were cultured as described above except with 75% female rat serum/25% Tyrode's as the culture serum. Following 2hr pre-incubation with D3T, FITC-Ab (100 μg/ml) was added to the culture medium in each culture bottle (Ambroso & Harris, 2012). Culture bottles were then incubated for 1 or 3 hours with treatment groups Control, D3T (10μM), VPA (600μM) or VPA + D3T (600μM + 10μM). Following incubation, conceptuses were rinsed in 50mM sodium phosphate buffer then pipetted into a 250μL drop where the VYS and EMB were separated allowing the extraembryonic fluid (EEF) to release into the sodium phosphate buffer. VYS and EMB were separately rinsed then added to tubes containing 250μL 0.1% Triton X-100. All samples were homogenized and then had a 20ul aliquot saved for BCA assay to determine protein content. Protein was precipitated through acidification with 750μL 6% TCA (w/v) for 1hr followed by centrifugation and separation of the pellet and supernatant. TCA soluble supernatants were combined with 1ml of 500nM Tris and 150μL of 1N NaOH to bring to pH of 8.8. TCA-insoluble pellets were dissolved with 150μL of 1N NaOH, vortexed and incubated for 1 hour. 1ml 500mM Tris, 150μL 1N NaOH, and 750μL 6% TCA were then added to both the acid soluble and insoluble samples. Culture media aliquots were collected in 250μL of 0.1% Triton X-100 (v/v), 750μL of 6% TCA with 1% SDS (v/v) and 150μL of 1N NaOH and processed as described above into TCA soluble and insoluble fractions. Fluorescence of all samples and blanks were measured

Author Manuscript Author Manuscript Author Manuscript Author Manuscript

in black polypropylene 96-well plate and read at an excitation wavelength of 495nm with 520nm emission on a SpectraMax Gemini XS (Molecular Devices; San Jose, CA). A standard curve of a 1:10000 dilution of FITC-Ab balanced for pH with 500nM Tris and 6% TCA was used for quantification.

2.7 RNA Extraction and qPCR

Treatment groups for qPCR and Western Blots included: Control, D3T (*in vitro*, 10μM), D3T (*in vivo*, 5mg/kg), VPA (600μM), and VPA + D3T (600μM + *in vitro* 10μM & 600μM + *in vivo* 5mg/kg). *In vivo* D3T dosing was administered on GD 7.5 through an IP injection of 100μL with a vegetable oil vehicle. *In vivo* dosing and culture conditions were performed as described above. Conceptuses were rinsed twice in HBSS before separation of embryo and visceral yolk sac. Tissues were saved in groups of 5 in 50μL RNALater (Invitrogen; Carlsbad, CA). RNA extraction was performed using the RNeasy kit according to manufacturer's instructions (Qiagen; Hilden, Germany). RNA concentration and quality were verified by Nanodrop (Thermo Fisher Scientific; Waltham, MA). RNA was synthesized into cDNA using the iScript cDNA Synthesis Kit (Bio-Rad; Hercules, CA) and prepared for quantitative real-time PCR using SYBR Green Detection Master Mix (SABiosciences; Frederick, MD) per the manufacturer's instructions in a StepOnePlus real-time PCR cycler (Applied Biosystems; Foster City, CA). All primers were purchased from Integrated DNA Technologies (Coralville, IA). β-actin was measured as a housekeeping gene for normalization purposes. Samples were analyzed using the ΔΔCt method and analyzed relative to the 0hr control. Samples were run in triplicate, n = 3. Genes of interest included Glutamate-cysteine ligase catalytic subunit (GCLC), Heme Oxygenase 1 (HO1), and NADPH dehydrogenase (quinone 1) (NQ01) which are all known downstream gene targets of Nrf2 activation (Alam et al., 1999; Venugopal & Jaiswal, 1996; Wild et al., 1999). The ß-actin (4970S) primary antibody was purchased from Cell Signaling Technology (Danvers, MA). NQO1 (ab28947), GCLC (ab190685), and HO1 (ab13248) primary antibodies were purchased from Abcam (Cambridge, UK). The secondary antibodies used were Alexa Fluor 680 donkey anti-mouse (175774) and 800 goat anti-rabbit (ab216773).

2.8 Western Blots

Conceptuses were rinsed twice in HBSS before separation of embryo and visceral yolk sac. Tissues were saved in 100μL RIPA buffer in groups of 4–6 then sonicated. Protein concentration was determined through BCA assay and equal amounts of protein were separated by 10% SDS-polyacrylamide gel electrophoresis using a PowerPac Basic electrophoresis unit (Bio-Rad; Hercules, CA) run at 80V and transferred onto nitrocellulose membranes. ß-actin (4970S) primary antibody was purchased from Cell Signaling Technology (Danvers, MA). NQO1 (ab28947), GCLC (ab190685), and HO1(ab13248) antibodies were purchased from Abcam (Cambridge, UK). The membranes were blocked with LiCor blocking buffer (LiCor Biosciences; Lincoln, NE) for 60 minutes at room temperature and then probed with the denoted primary antibodies diluted 1:500 in PBS with 0.1% Tween 20 (Thermo Fisher Scientific; Waltham, MA) at 4°C overnight. The next day, membranes were probed with fluorescent Alexa Fluor secondary antibodies (LiCor Biosciences; Lincoln, NE) at room temperature for 90 minutes. Membranes were imaged on an Odyssey CLx scanner (LiCor Biosciences; Lincoln, NE) and quantified by expression of

Author Manuscript Author Manuscript Author Manuscript Author Manuscript

the desired protein relative to the actin loading control. Western blot and qPCR data are expressed as the mean ± SEM.

2.9 Statistical Analysis

To determine statistical significance for thiol concentrations, redox potential and histiotrophic nutrition, a one-way ANOVA was calculated within each timepoint across treatment groups. A confidence level of 95% (α=0.05) was utilized as a threshold for statistical significance. Significant ANOVA results underwent Tukey's post-hoc test to determine the significant group(s). Statistics were performed in Excel using the Real Statistics Resource Pack add-in and where applicable are reported as mean ± standard error with $p<0.05$ indicated with an asterisk. Statistical analysis of qPCR and western blots was performed using Prism v7.00 software (Graphpad Software Inc.; San Diego, CA). Statistical comparisons were made using a one-way analysis of variance (ANOVA) followed by Dunnett's post hoc test with statistical significance denoted as a $p < 0.05$. Asterisks denote statistical significance compared to the control.

3. Results

The described experiments were conducted to evaluate the spatial and temporal baseline redox steady states of the organogenesis stage mouse conceptus under control and VPA and/or D3T perturbed conditions. Measurements of GSH, GSSG, Cys, and CySS across embryonic time and space were used to calculate total glutathione (GSH + 2GSSG) and total cysteine (Cys + 2CySS) as well as the corresponding redox potential (E_h) for each thiol pair. Finally, the histiotrophic nutrition assay measured protein uptake via receptor mediated endocytosis in the VYS across early organogenesis to determine whether an association exists between reduced GSH or Cys concentrations and decreased histiotrophic nutrition under VPA-treated conditions.

3.1 Total Glutathione and Total Cysteine

Total glutathione (GSH + 2xGSSG) and total cysteine (Cys + 2CySS) concentrations in tissue and fluid compartments are displayed for each 2hr interval across the 24hr time course as heat maps in order to provide a qualitative context of changes in soluble thiol levels over developmental time (Figures 1, 2, and 3). This analysis shows concentrations of total (oxidized and reduced) thiols. Changes in oxidation states for the respective redox pairs are shown below as their respective redox potentials (E_h) as bubble diagrams in Figure 4. The quantitation of soluble thiols (GSH and Cys) in the developing EMB and VYS has historically been accompanied by a higher than expected degree of variability (Harris et al., 2013, 2015; Jilek et al., 2015). Standard error for EMB total glutathione in this study ranged from 128 to 2290μM across the 24hr developmental time course based on a relatively small sample size of three per timepoint and treatment (Figure 1). This variability is visualized as a histogram of total glutathione with standard error bars in Figure 1 to illustrate the need for a more qualitative, pattern-based visualization through the use of heat maps for the subsequent figures. Aside from a determination of "statistical significance" there is no established benchmark value of altered thiol concentration or redox potential that, when reached, confirms that a deleterious consequence or manifestation of toxicity will occur. By

Author Manuscript Author Manuscript Author Manuscript Author Manuscript

displaying redox potential and total soluble thiol concentrations as a heat map, we are able to visualize the relative patterns and trends of change in antioxidant potential and cellular redox status in a temporal and spatial manner across tissue and fluid compartments.

Concentrations of total glutathione fluctuate naturally in the control VYS between 1400 and 5600μM across the time course with highs at 6hr and 14hr and a low at 16hr. Control EMB total glutathione drops to its lowest levels at 10hr and 12hr followed by a peak at 14hr. Total glutathione concentrations in the YSF and AF compartments are considerably lower compared to tissues with a much narrower range of variation, fluctuating between 5μM and 120μM, showing their highest concentrations during the first 8–10 hours with peaks at 4hr (Figure 2). In contrast to the control values of total glutathione, VPA treatment caused noticeably higher levels of total glutathione from 2–4, 8–10, and 18hrs in the VYS and 4, 16, and 22hrs in the EMB. The only noticeable increase in total glutathione in the fluid compartments following VPA treatment was at 18hrs in the AF.

Total cysteine concentrations range from 127–936μM in control EMB and 107–1152μM in the VYS. Similar to total glutathione, the concentration of total cysteine in the fluid compartments is much lower than in the tissues with a control concentration of 7–199μM in YSF and 13–218μM in the AF. In the tissues, VPA causes elevated levels of total cysteine compared to the control at 12 and 22hrs in the VYS and 4 and 22hrs in the embryo. The fluid compartments show greater sensitivity to VPA with more periods of increased total cysteine from 2, 20, 24hrs in the YSF and 8, 16, 22–24hrs in the AF.

3.2 Thiol Pair Redox Potentials

Redox potential (E_h) measures the steady state balance between oxidized and reduced counterparts of a redox active thiol couple such as GSH and GSSG or Cys and CySS. Figure 4 visualizes E_h values as a heat map across developmental time and space for each of these redox pairs. Across all treatment groups, the YSF and AF compartments exhibited a more oxidized E_h than the tissue compartments for both GSH:GSSG and Cys:CySS. In the control, compartmental GSH E_h ranged from −168 to −208mV in the VYS, −172 to −229mV in the EMB, −98 to −136mV in the YSF and −118 to −149mV in the AF. VPA treatment causes a distinct oxidation event in all tissues and fluid compartments in the GSH:GSSG redox potential at 4, 10 and 14hrs compared to the control, but at 6, 8, and 20hrs, nearly identical redox profiles were seen across all tissues. Co-treatment with D3T and VPA did not maintain a control level oxidation profile, and in some cases, such as at 20hrs, the co-treatment lead to more oxidation than seen in any of the other treatment groups with a compartmental range of −111 to −156mV compared to −129 to −229mV in the control. Across the 24 hours of sampling, all VYS showed a trend toward becoming increasingly reduced. EMB fluctuated between −180 to −220mV with a low of −230 and a high of −155mV both at 20 hours in the control and VPA + D3T group respectively for the GSH:GSSG redox potential. AF and YSF GSH:GSSG redox potential trended toward becoming more reduced by the end of the time course. Thus, in spite of considerable variation in steady state E_h during the GD8 segment of the time course, all tissues and fluids show progressive reduction as growth and development proceeds during organogenesis.

Author Manuscript Author Manuscript Author Manuscript Author Manuscript

The Cys:CySS redox potential was consistently more oxidized than the GSH:GSSG redox potential (Figure 4). This more oxidized Cys:CySS redox potential was expected due to Cys being predominately found in its oxidized form, CySS, in extracellular spaces compared to the reduced form which is found at much lower concentrations intracellularly (McBean, 2017). Control values of the Cys:CySS redox potential ranged from −72 to −147mV in the VYS, −45 to −149mV in the EMB, −31 to −91mV in the YSF, and −49 to −113mV in the AF. At 12 hours most treatment groups showed a reduction in the VYS Cys:CySS redox potential followed by a reversion to oxidation at 14hrs. At 24hrs, all tissues and fluids showed a highly oxidized Cys:CySS redox potential. Compared to the control VPA treatment lead to visible reduction in all tissues at 18 and 22hrs which was also seen in most tissues in the VPA + D3T group at the same time points.

Whole conceptus redox potential measurements for GSH:GSSG were more reduced than those of isolated EMBs and VYSs at the corresponding time points (Figure 5). The pattern of reduction and oxidation over time, however, is similar between whole conceptus, EMB, and VYS which indicates that while the time-sensitive manipulation of conceptuses to separate tissues may cause slight artifactual oxidation, the patterns of increased and decreased oxidation remain consistent.

MEHP and TBHQ treatments were administered as positive controls at 4 and 22hrs. Both compounds have shown the capacity to act as oxidants in developmental models of mouse or zebrafish embryos (Sant, et al., 2016b; Sant et al., 2017). In the VYS and EMB, the VPA GSH:GSSG redox potential was statistically more reduced ($p<0.05$) following 4 and 22hrs of treatment than either dose of MEHP or TBHQ (Figure 6). The YSF and AF showed no statistical difference in GSH:GSSG redox potential between VPA, MEHP, or TBHQ at 4 or 22 hours. In all tissues and fluid compartments, the low and high dose of MEHP or TBHQ showed no statistical difference from each other in their effect on GSH:GSSG redox potential.

3.3 Nrf2 Pathway Activation by D3T

To determine whether D3T was properly inducing the Nrf2 antioxidant response, during the 2-hour *in vitro* pre-treatment, RT-qPCR of three downstream marker genes of Nrf2 were evaluated (Figure 7). NQO1, a Nrf2-induced antioxidant, increased significantly in gene expression following both *in vitro* and *in vivo* D3T treatment in the embryo and in EMB and VYS in combination with *in* vitro VPA. HO1, another Nrf2 induced antioxidant, showed a significant increase in gene expression in the EMB for all groups treated with D3T and in the VYS in all groups treated with D3T except *in vivo* D3T alone. GCLC, a rate-limiting enzyme for glutathione synthesis showed no significant increases in gene expression, although the *in vivo* and *in vitro* VPA + D3T combination treatments were trending toward significance in both tissues. There was no difference between VPA treated and control EMB or VYS in any of the three genes.

To complement gene expression data, western blots were performed to evaluate protein expression of the same three downstream Nrf2 targets (Figure 8). NQO1 protein expression was increased in the EMB following *in vivo* D3T dosing as well as in EMB and VYS following *in vivo* or *in vitro* D3T in combination with *in vitro* VPA. HO1 protein expression

Author Manuscript Author Manuscript Author Manuscript Author Manuscript

was significantly elevated in EMB and VYS following in vitro *D3T dosing and in the EMB only* after both VPA+D3T combination treatments. GCLC showed elevated protein expression in the VYS and EMB following *in vitro* D3T, *in vivo* D3T and *in* vitro VPA + D3T dosing, but only showed elevated protein expression in the VYS following *in vivo* D3T + *in vitro* VPA. Unlike in the gene expression data, VPA alone caused moderate increases in protein expression of NQO1 and HO1.

3.4 Histiotrophic Nutrition

The total histiotrophic clearance rate of FITC-Ab was decreased compared to the control after 1 and 3hrs exposure to VPA and VPA+D3T (Figure 9). After 1hr, control clearance was 102μL media/mg/hr compared to 62 and 52μL/mg/hr in VPA and VPA+D3T respectively. Similarly, at 3hrs, control clearance was 40μL media/mg/hr with VPA and VPA+D3T clearance at 32 and 25μL/mg/hr. Total FITC-Ab clearance at 3hrs was also reduced in VPA and VPA+D3T treated groups with total clearance of 120μL/mg in the Control compared to 97 and 74μL/mg in the VPA and VPA+D3T treatment groups. The majority of FITC label was detected in the VYS and the EEF with only trace amounts reaching the embryo. In all treatment groups and time points the total uptake rate of acid soluble (degraded protein) and acid insoluble (intact protein) was roughly equal, but with the majority of acid soluble uptake in the VYS and the majority of insoluble uptake found in the EEF.

4. Discussion

The aim of the 24-hour time course was to determine whether VPA perturbed the cellular redox environment during the period of mouse NTC in a spatially and temporally specific manner. The stated hypothesis considered that if VPA's mechanism of action involved increased cellular oxidation, it would cause an elevated GSH:GSSG redox potential and deplete GSH concentrations in all tissues and fluids across the time course. Redox profiles based on the GSH/GSSG and Cys/CySS redox couples did not show sustained oxidation by VPA across the time course of early organogenesis. Observed patterns of spatial and temporal fluctuations in soluble thiol antioxidant status may serve to indicate specific targets and periods of enhanced sensitivity for chemical and environmental insults. The logic behind using a more generalized visualization of cellular redox states during organogenesis, measured from soluble thiols (GSH and Cys) and their respective redox potentials as heat maps, is based on considerations related to the need to visualize patterns of thiol oxidation and reduction as an ontogeny. Broad experience with developmental toxicology studies and rodent whole embryo culture reveal that any detailed sampling of individual litters will exhibit a spectrum of responses to developmental toxicants, such as VPA, that range from very high sensitivity to very high resistance in terms of malformations, functional deficits and embryo mortality. This is the basis for evaluating developmental toxicant effects by litter, rather than averaging individual embryo effects from litters of varying sensitivity (Hardy & Stedeford, 2008). The randomization method used in these experiments mixes conceptuses from many different litters that, individually, represent the entire range of sensitivity and resistance across a broad population spectrum. This conservative approach is expected to minimize the contribution of a few highly sensitive or resistant litters and show a general ontogeny of redox shifts. Different types of chemical agents such as the positive

Author Manuscript Author Manuscript Author Manuscript Author Manuscript

controls TBHQ and MEHP are shown to be more responsive when taken from a much smaller total number/subset of litters.

In both whole conceptus and compartmental tissue and fluids, VPA did not consistently demonstrate the capacity to act as an oxidant through alterations of GSH and Cys concentrations. However, there were separate periods of oxidation seen for individual tissues and three time points (4, 10, and 14 hours) where all four embryonic compartments showed an oxidizing GSH:GSSG redox potential compared to the control tissues at the same time period (Figure 4). These two later time points, 10 and 14hrs, could be related to the morphological milestones related to neural tube closure that occur during the last quarter of GD8. In late GD8 when the embryo is in the stage of 15.4–17.7 somites, neural tube development completes two closures at the telencephalic neuropore followed by the metencephalic neuropore with average timing of about 2hrs between these events (Sakai, 1989). The oxidation seen across the 4 embryonic compartments at 10 and 14hrs, could be indicative of VPA's disruption of specific aspects of the neural tube closure process, although it is still unknown whether neural fold elevation or apical fusion is involved. The earlier time point of VPA-induced oxidation at 4hrs occurred during the time period of heartbeat activation which occurs between the 4 and 8 somite stage around mid-GD8 (Nishii & Shibata, 2006). Therefore, it is possible that some of the timed elevations in the GSH:GSSG redox potential could be linked to other morphological or physiological development milestones during mouse organogenesis.

Positive controls, TBHQ and MEHP, are known oxidants with MEHP also being implicated in causing NTDs (Sant et al., 2016b). TBHQ and MEHP produced statistically significant levels of oxidation in the EMB and VYS but not in the fluid compartments supporting the idea that oxidation responses in the mouse conceptus may be tissue dependent. The MEHP results confirm previous results indicating that a 12hr exposure to MEHP increased GSH E_h in the EMB but not VYS (Sant et al., 2016b). Despite not showing significant evidence for VPA's oxidative potential, this study's 2hr sampling windows provided more finely timed points of measurement than seen in most redox studies illustrating that thiol concentrations are in constant flux and that stationary measurements from a single time point are not enough to capture the dynamic nature of the redox control of development. When compared to redox profiles of organogenesis stage zebrafish development (18–24hpf), the control tissues and fluids show a similar pattern of shifting toward a more reduced GSH potential compared to the earlier stages of organogenesis (Timme-Laragy et al., 2013). Redox shifts encompassed in the 24-hour time course could also be significant in understanding physiological and structural birth defects related to the heart, eye, ear and limbs as these organs all achieve significant developmental milestones during the same time period as neural tube closure including heartbeat activation, limb bud development, optic cup and otic vesicle formation (Harris, 2012).

While there is evidence to demonstrate VPA's actions as an oxidant, there are also studies that indicate that under some conditions VPA may have the capacity to act as an antioxidant. In a rat model of sepsis, treatment with VPA reduced oxidative injury as measured by decreased levels of ROS and malondialdehyde (MDA) as well as increased levels of GSH, and superoxide dismutase (SOD) in myocardial tissue (Shi et al., 2019). Similarly, a mouse

Author Manuscript Author Manuscript Author Manuscript Author Manuscript

model of sepsis, found that VPA reduced levels of MDA and myeloperoxidase, while increasing levels of GSH and SOD indicating an overall reduction of oxidation markers in renal tissue (Liu et al., 2014). Human neuroblastoma SH-SY5Y cells treated with VPA for 1 week have been shown to increase glutathione levels compared to controls, while maintaining lactate dehydrogenase levels (LDH) and in some cases reducing oxidation caused by Rotenone and H_2O_2 (J. Cui et al., 2007; Lai et al., 2006). Finally, VPA was shown to eliminate oxidative protein lesions found in a mouse model mimicking the neurodegenerative condition, X-linked adrenoleukodystrophy through inducing the expression of a peroxisomal transporter related to a transporter that loses function through the disease (Fourcade et al., 2010). Together, these studies could help explain why VPA did not cause consistent oxidation across the developmental time course.

The discordant research findings related to VPA's redox manipulation make it imperative that VPA be evaluated under conditions that most specifically relate to the outcome of interest to determine whether its actions are more pro- or antioxidant in nature. Recent findings related to oxidative post-translational modification of protein Cys in young and old mice has indicated that protein redox changes are often specific to tissue and age (Xiao et al., 2020). This research is particularly relevant to development as it is one of the most dynamic periods of life for programmed oxidation events (Hansen et al., 2020). The hypothesis that VPA would consistently elevate oxidation levels across organogenesis as measured through total thiol concentrations and redox potentials in conjunction with causing morphological abnormalities was not supported. It is possible, however, that these findings may have been masked by the intricate timeline of morphological changes that occur in addition to NTC during this time period and the use of the broad developmental tissue and fluid compartments to study the spatiality of redox without the ability to differentiate between the many developing organ systems. Additionally, although VPA is known to suppress activation of the Nrf2 antioxidant system and did not show increases in downstream Nrf2 gene and protein targets, HO1, GCLC, or NQO1 compared to the control, the primary transcription factor regulating basal antioxidant levels throughout development is Nrf1 which as evidenced by the similarities between control and VPA-treated qPCR and western blot data remains intact (Palsamy et al., 2014; Raghunath et al., 2018). It is therefore possible that basal levels of GSH synthesized through activation of the Nrf1 pathway could be sufficient to react to minor oxidation shifts caused by VPA without noting extended periods of redox imbalance that could be captured by 2hr windows of the GSH:GSSG E_h. Alternatively, the findings of Xiao, et al. support the idea that naturally occurring and VPA-perturbed developmental redox signaling may be occurring primarily at the protein level independent of GSH redox states through oxidative post-translational modification of Cys residues (Xiao et al., 2020). This same reasoning may also resolve the limited changes in cellular redox profile following pre-treatment of conceptuses with D3T. Potential changes to the oxidation state of the developmental proteome would allow for natural and VPA-perturbed development to proceed with more targeted oxidation events that could be more time specific to protein pathways implicated in development of specific tissues and organs than could be achieved through GSH levels alone.

Pre-treatment of samples with D3T was intended to induce the Nrf2 antioxidant response prior to the challenge with suspected oxidant VPA based on numerous previous studies that

Author Manuscript Author Manuscript Author Manuscript Author Manuscript

have demonstrated D3T's ability to increase antioxidant concentrations and decrease markers of oxidative stress in both *in vivo* mouse and *in vitro* mouse cell models (Y. Cui et al., 2018; Kuo et al., 2017; Wang et al., 2017). Total glutathione concentration showed limited elevation in GSH from 4–10hrs in the VYS with no apparent change in the other tissues or in redox potential following 2hr *in vitro* D3T treatment. Despite seeing only limited time and tissue specific changes in total glutathione, *in vitro* D3T dosing did increase gene expression of HO1 in VYS and EMB and NQO1 in the embryo with protein expression showing increased GCLC and HO1 in both VYS and EMB (Figures 7 and 8). GD7.5 *in vivo* IP D3T data also proved effective at increasing gene expression of NQO1 and HO1 in the EMB and increasing protein expression of NQO1 in the embryo and GCLC in EMB and VYS but was not more effective than the shorter *in vitro* dosing indicating equivalence between these two dosing regimens. This data suggests that the redox activity of D3T through the Nrf2 pathway is activated through *in vitro* or *in vivo* pre-treatment, but that the downstream consequences of this induction are not seen through GSH measurements and may instead be promoting other downstream Nrf2 pathways. Additionally, the tissue selectivity seen with total glutathione elevation in the VYS that is absent in the EMB as well as the gene expression elevation of NQO1 in the EMB but not the VYS could indicate tissue differences in distribution of Nrf2 ARE targets or differences in Keap1 oxidation patterns that would affect Nrf2 nuclear translocation. There are four classes of ARE enhancer regions with 2 of these classes (I and II) being induced by Nrf2 as a transcription factor. Within these classes and even between ARE sequences for the same gene, there are known single nucleotide polymorphisms (SNPs) which have been shown to affect Nrf2 binding affinity (Raghunath et al., 2018). Timing of cell and tissue differentiation throughout development and tissue specific distribution of these ARE SNP varieties could therefore lead to differential antioxidant responses through the Nrf2 pathway over developmental time and space. Tissue-specific responses of Nrf2 gene GCLC were also noted in the EMB and VYS of post-implantation rat conceptuses where on both GD 10 and 11 (corresponding to mouse GD 8 and 9), concentrations of GCLC activity was two to three times higher in the VYS (Hansen et al., 2004).

It was predicted that co-treatment with VPA and D3T would decrease the oxidative effects of VPA alone, however as seen through the GSH:GSSG E_h and histiotrophic nutrition, there were several instances where the co-treatment caused an exacerbation of VPA's effects. Similar results were seen in a study of the oxidative effects of advanced glycation end products (AGE) on SH-SY5Y cells where it was seen that while treatment of the cells with only D3T caused no change in cell viability or ROS production, co-treatment with AGE and D3T lead to a decrease in viability and increase in ROS beyond what was seen with AGE treatment alone (Stochelski et al., 2019). This potentiation effect caused by D3T was attributed to an elevation of the Nrf2 associated gene G6PD and a decrease in glutathione reductase activity (Stochelski et al., 2019). Based on the RT-qPCR and western blot data, VPA + D3T treatment showed a strong Nrf2 induction for HO1, NQO1 and GCLC. It is therefore possible that the combination of VPA and D3T may be acting similarly through a potentiation effect, although unlike AGE, VPA did not show evidence of activating the Nrf2 pathway independently.

Author Manuscript Author Manuscript Author Manuscript Author Manuscript

Histiotrophic nutrition data suggests that VPA may slow the rate of uptake of proteins and essential amino acids during early organogenesis. Histiotrophic clearance was measured through uptake of FITC-Ab which was decreased following VPA exposure at both 1 and 3hrs, which could indicate a delay in uptake of essential amino acids for protein synthesis and redox regulation through glutathione synthesis. This pattern of decreased uptake was seen in both acid soluble and insoluble samples, as well as across the three developmental compartments of EMB, VYS, and EEF. Combination treatment with VPA + D3T had a slower rate of histiotrophic uptake compared to VPA alone, whereas D3T by itself showed little change in rate of uptake. In addition to rate of uptake being slowed in VPA and VPA + D3T treatment groups, the total uptake of FITC-Ab across the 3hr experimental period was also decreased compared to the control and D3T alone. Other developmental toxins, such as ethanol, have also been shown to impact histiotrophic nutrition uptake by leading to significantly reduced clearance following 3 hours of exposure in organogenesis-stage rat conceptuses (Jilek et al., 2015). In mouse conceptuses, oxidant MEHP has also been shown to reduce histiotrophic clearance after 3 hours at a dose of 250 μg/mL (Sant et al., 2016a). Both of these previous studies measured changes in clearance rate over 3hrs on GD9, so the assessment of VPA's effect on its histiotrophic nutrition during early-mid GD8 is unique. Compared to the MEHP and ethanol studies, there was a much higher proportion of total uptake from the acid insoluble, intact protein, fraction in both control and VPA treated samples which may be attributable to the earlier time point of analysis.

Comparing histiotrophic uptake rate at 1 and 3hrs to the total thiol and redox potential at 2 and 4hrs does not indicate a depletion of glutathione due to lower amino acid supply caused by VPA's slowed histiotrophic uptake. However, there is a slight decrease in total glutathione around 8–10hrs in the EMB and 10hrs in the VYS and EMB which could indicate the delayed effects of decreased amino acid uptake (Figures 1 and 2). Total cysteine concentrations are lower after 2hr VPA exposure in the EMB and VYS but higher in the YSF and AF (Figure 3). The decreased total cysteine after 2hr VPA exposure in the tissue compartments could be indicative of a combinatorial effect of reduced amino acid uptake through histiotrophic nutrition as well as increased glutathione synthesis evidenced by higher total glutathione levels at 2hrs in EMB and VYS compared to the control.

5. Conclusions

Overall, VPA treatment caused fewer perturbations to the organogenesis-stage mouse total GSH concentrations, total Cys concentrations and thiol pair redox potentials than expected. However, there were still distinct periods of oxidation produced by VPA that were time and tissue specific which, along with a potential disruption in histiotrophic nutrition, could affect maintenance of a developmentally appropriate redox state. Co-treatment of the conceptuses with D3T did not consistently reduce oxidation caused by VPA or retain control level histiotrophic nutrition uptake rates, suggesting that further study of this combination treatment is warranted to understand the importance of Nrf2 induction on VPA outcomes. Additionally, the carefully timed measurement of cellular redox in the control across 24hrs of organogenesis demonstrated that even in properly developing conceptuses, redox is in a natural state of fluctuation that differs across developmental time and space thereby underlining the importance of time course evaluation to understand redox mechanisms of

Author Manuscript Author Manuscript Author Manuscript Author Manuscript

development. These results suggest that further testing of VPA and other potentially teratogenic compounds and therapeutic agents for safety during pregnancy should be conducted over time within several embryonic tissue targets as singular, one time, sampling of whole conceptuses may not be a valid measure of drug safety due to the potential for developmental interruption to be specific to the tissue and timing of exposure. While the results of this study indicate that VPA may not act as a consistent oxidant under the traditional dogma of oxidative stress through manipulating cellular total GSH and its redox potential, there is a growing body of evidence that oxidative post-translational modifications of protein Cys residues may be differentially affected by tissue and age which could be applicable to development and neural tube closure. Further exploration of the relationship between protein redox status and VPA treatment during mouse organogenesis is needed to understand whether VPA may act through a pathways of oxidative post-translational protein modifications that could influence protein structure or function and developmental progression.

Acknowledgments

Funding: This work was supported by the National Institutes of Health [NIH T32 ES007062] and a Faculty Research Grant from the University of Michigan Office of Research and the Michigan School of Public Health. These funding sources had no role in study design, data collection and analysis, or writing and publication.

References

Ahangar N, Naderi M, Noroozi A, Ghasemi M, Zamani E, & Shaki F (2017). Zinc Deficiency and Oxidative Stress Involved in Valproic Acid Induced Hepatotoxicity: Protection by Zinc and Selenium Supplementation. Biological Trace Element Research, 179(1), 102–109. 10.1007/s12011-017-0944-z [PubMed: 28124216]

Alam J, Stewart D, Touchard C, Boinapally S, Choi AMK, & Cook JL (1999). Nrf2, a Cap'n'Collar Transcription Factor, Regulates Induction of the Heme Oxygenase-1 Gene. Journal of Biological Chemistry, 274(37), 26071–26078. 10.1074/jbc.274.37.26071

Ambroso J, & Harris C (2012). Assessment of Histiotrophic Nutrition Using Fluorescent Probes. In Harris C & Hansen JM (Eds.), Developmental Toxicology (Vol. 889, pp. 407–423). Humana Press. 10.1007/978-1-61779-867-2_25

Bruckner A, Lee YJ, O'Shea KS, & Henneberry RC (1983). Teratogenic effects of valproic acid and diphenylhydantoin on mouse embryos in culture. Teratology, 27(1), 29–42. 10.1002/tera.1420270106 [PubMed: 6405496]

Burton GJ, Hempstock J, & Jauniaux E (2001). Nutrition of the Human Fetus during the First Trimester—A Review. Placenta, 22, S70–S77. 10.1053/plac.2001.0639 [PubMed: 11312634]

Burton Graham J., Watson AL, Hempstock J, Skepper JN, & Jauniaux E (2002). Uterine Glands Provide Histiotrophic Nutrition for the Human Fetus during the First Trimester of Pregnancy. The Journal of Clinical Endocrinology & Metabolism, 87(6), 2954–2959. 10.1210/jcem.87.6.8563 [PubMed: 12050279]

Chaudhary S, Ganjoo P, Raiusddin S, & Parvez S (2015). Nephroprotective activities of quercetin with potential relevance to oxidative stress induced by valproic acid. Protoplasma, 252(1), 209–217. 10.1007/s00709-014-0670-8 [PubMed: 25000991]

Cui J, Shao L, Young LT, & Wang J-F (2007). Role of glutathione in neuroprotective effects of mood stabilizing drugs lithium and valproate. Neuroscience, 144(4), 1447–1453. 10.1016/j.neuroscience.2006.11.010 [PubMed: 17184924]

Cui Y, Ma S, Zhang C, Li D, Yang B, Lv P, Xing Q, Huang T, Yang GL, Cao W, & Guan F (2018). Pharmacological activation of the Nrf2 pathway by 3H-1, 2-dithiole-3-thione is neuroprotective in a mouse model of Alzheimer disease. Behavioural Brain Research, 336, 219–226. 10.1016/j.bbr.2017.09.011 [PubMed: 28887195]

Author Manuscript Author Manuscript Author Manuscript Author Manuscript

De Marco P, Merello E, Cama A, Kibar Z, & Capra V (2011). Human neural tube defects: Genetic causes and prevention. BioFactors, 37(4), 261–268. 10.1002/biof.170 [PubMed: 21674647]

Dong J, Sulik KK, & Chen S (2008). Nrf2-Mediated Transcriptional Induction of Antioxidant Response in Mouse Embryos Exposed to Ethanol *in vivo*: Implications for the Prevention of Fetal Alcohol Spectrum Disorders. Antioxidants & Redox Signaling, 10(12), 2023–2033. 10.1089/ars.2007.2019 [PubMed: 18759561]

Fourcade S, Ruiz M, Guilera C, Hahnen E, Brichta L, Naudi A, Portero-Otín M, Dacremont G, Cartier N, Wanders R, Kemp S, Mandel JL, Wirth B, Pamplona R, Aubourg P, & Pujol A (2010). Valproic acid induces antioxidant effects in X-linked adrenoleukodystrophy. Human Molecular Genetics, 19(10), 2005–2014. 10.1093/hmg/ddq082 [PubMed: 20179078]

Greene NDE, & Copp AJ (2014). Neural Tube Defects. Annual Review of Neuroscience, 37(1), 221–242. 10.1146/annurev-neuro-062012-170354

Grosse SD, Berry RJ, Mick Tilford J, Kucik JE, & Waitzman NJ (2016). Retrospective Assessment of Cost Savings From Prevention. American Journal of Preventive Medicine, 50(5), S74–S80. 10.1016/j.amepre.2015.10.012 [PubMed: 26790341]

Hansen JM (2006). Oxidative stress as a mechanism of teratogenesis. Birth Defects Research Part C: Embryo Today: Reviews, 78(4), 293–307. 10.1002/bdrc.20085

Hansen JM, Jones DP, & Harris C (2020). The Redox Theory of Development. Antioxidants & Redox Signaling, 32(10), 715–740. 10.1089/ars.2019.7976 [PubMed: 31891515]

Hansen JM, Lee E, & Harris C (2004). Spatial activities and induction of glutamate-cysteine ligase (GCL) in the postimplantation rat embryo and visceral yolk sac. Toxicological Sciences: An Official Journal of the Society of Toxicology, 81(2), 371–378. 10.1093/toxsci/kfh154 [PubMed: 15115889]

Hardy M, & Stedeford T (2008). Use of the Pup as the Statistical Unit in Developmental Neurotoxicity Studies: Overlooked Model or Poor Research Design? Toxicological Sciences, 103(2), 409–410. 10.1093/toxsci/kfn036 [PubMed: 18463102]

Harris C (2012). Rodent Whole Embryo Culture. In Harris C & Hansen JM (Eds.), Developmental Toxicology (Vol. 889, pp. 215–237). Humana Press. 10.1007/978-1-61779-867-2_13

Harris C, & Hansen JM (2012a). Oxidative Stress, Thiols, and Redox Profiles. In Harris C & Hansen JM (Eds.), Developmental Toxicology (Vol. 889, pp. 325–346). Humana Press. 10.1007/978-1-61779-867-2_21

Harris C, & Hansen JM (2012b). Nrf2-Mediated Resistance to Oxidant-Induced Redox Disruption in Embryos. Birth Defects Research Part B: Developmental and Reproductive Toxicology, 95(3), 213–218. 10.1002/bdrb.21005 [PubMed: 22495766]

Harris C, Jilek JL, Sant KE, Pohl J, Reed M, & Hansen JM (2015). Amino acid starvation induced by protease inhibition produces differential alterations in redox status and the thiol proteome in organogenesis-stage rat embryos and visceral yolk sacs. The Journal of Nutritional Biochemistry, 26(12), 1589–1598. 10.1016/j.jnutbio.2015.07.026 [PubMed: 26365578]

Harris C, Shuster DZ, Roman Gomez R, Sant KE, Reed MS, Pohl J, & Hansen JM (2013). Inhibition of glutathione biosynthesis alters compartmental redox status and the thiol proteome in organogenesis-stage rat conceptuses. Free Radical Biology and Medicine, 63, 325–337. 10.1016/j.freeradbiomed.2013.05.040 [PubMed: 23736079]

Jilek JL, Sant KE, Cho KH, Reed MS, Pohl J, Hansen JM, & Harris C (2015). Ethanol Attenuates Histiotrophic Nutrition Pathways and Alters the Intracellular Redox Environment and Thiol Proteome during Rat Organogenesis. Toxicological Sciences, 147(2), 475–489. 10.1093/toxsci/kfv145 [PubMed: 26185205]

Jones DP (2002). Redox potential of GSH/GSSG couple: Assay and biological significance. In Methods in Enzymology (Vol. 348, pp. 93–112). Elsevier. 10.1016/S0076-6879(02)48630-2 [PubMed: 11885298]

Komulainen T, Lodge T, Hinttala R, Bolszak M, Pietilä M, Koivunen P, Hakkola J, Poulton J, Morten KJ, & Uusimaa J (2015). Sodium valproate induces mitochondrial respiration dysfunction in HepG2 in vitro cell model. Toxicology, 331, 47–56. 10.1016/j.tox.2015.03.001 [PubMed: 25745980]

Author Manuscript Author Manuscript Author Manuscript Author Manuscript

Kuo P-C, Yu I-C, Scofield BA, Brown DA, Curfman ET, Paraiso HC, Chang F-L, & Yen J-H (2017). 3 H −1,2-Dithiole-3-thione as a novel therapeutic agent for the treatment of ischemic stroke through Nrf2 defense pathway. Brain, Behavior, and Immunity, 62, 180–192. 10.1016/j.bbi.2017.01.018

Lai JS, Zhao C, Warsh JJ, & Li PP (2006). Cytoprotection by lithium and valproate varies between cell types and cellular stresses. European Journal of Pharmacology, 539(1–2), 18–26. 10.1016/j.ejphar.2006.03.076 [PubMed: 16678157]

Liu Z, Li Y, Chong W, Deperalta DK, Duan X, Liu B, Halaweish I, Zhou P, & Alam HB (2014). Creating a Prosurvival Phenotype Through a Histone Deacetylase Inhibitor in a Lethal Two-Hit Model: Shock, 41(2), 104–108. 10.1097/SHK.0000000000000074 [PubMed: 24430491]

McBean G (2017). Cysteine, Glutathione, and Thiol Redox Balance in Astrocytes. Antioxidants, 6(3), 62. 10.3390/antiox6030062

Nishii K, & Shibata Y (2006). Mode and determination of the initial contraction stage in the mouse embryo heart. Anatomy and Embryology, 211(2), 95–100. 10.1007/s00429-005-0065-x [PubMed: 16320070]

Palsamy P, Bidasee KR, & Shinohara T (2014). Valproic acid suppresses Nrf2/Keap1 dependent antioxidant protection through induction of endoplasmic reticulum stress and Keap1 promoter DNA demethylation in human lens epithelial cells. Experimental Eye Research, 121, 26–34. 10.1016/j.exer.2014.01.021 [PubMed: 24525405]

Raghunath A, Sundarraj K, Nagarajan R, Arfuso F, Bian J, Kumar AP, Sethi G, & Perumal E (2018). Antioxidant response elements: Discovery, classes, regulation and potential applications. Redox Biology, 17, 297–314. 10.1016/j.redox.2018.05.002 [PubMed: 29775961]

Sakai Y (1989). Neurulation in the mouse: Manner and timing of neural tube closure. The Anatomical Record, 223(2), 194–203. 10.1002/ar.1092230212 [PubMed: 2712345]

Sant KE, Dolinoy DC, Jilek JL, Sartor MA, & Harris C (2016b). Mono-2-ethylhexyl phthalate disrupts neurulation and modifies the embryonic redox environment and gene expression. Reproductive Toxicology, 63, 32–48. 10.1016/j.reprotox.2016.03.042 [PubMed: 27167697]

Sant KE, Dolinoy DC, Jilek JL, Shay BJ, & Harris C (2016a). Mono-2-ethylhexyl phthalate (MEHP) alters histiotrophic nutrition pathways and epigenetic processes in the developing conceptus. The Journal of Nutritional Biochemistry, 27, 211–218. 10.1016/j.jnutbio.2015.09.008 [PubMed: 26507544]

Sant KE, Hansen JM, Williams LM, Tran NL, Goldstone JV, Stegeman JJ, Hahn ME, & Timme-Laragy A (2017). The role of Nrf1 and Nrf2 in the regulation of glutathione and redox dynamics in the developing zebrafish embryo. Redox Biology, 13, 207–218. 10.1016/j.redox.2017.05.023 [PubMed: 28582729]

Schafer FQ, & Buettner GR (2001). Redox environment of the cell as viewed through the redox state of the glutathione disulfide/glutathione couple. Free Radical Biology and Medicine, 30(11), 1191–1212. 10.1016/S0891-5849(01)00480-4 [PubMed: 11368918]

Shi X, Liu Y, Zhang D, & Xiao D (2019). Valproic acid attenuates sepsis-induced myocardial dysfunction in rats by accelerating autophagy through the PTEN/AKT/mTOR pathway. Life Sciences, 232, 116613. 10.1016/j.lfs.2019.116613 [PubMed: 31265853]

Stochelski MA, Wilmanski T, Walters M, & Burgess JR (2019). D3T acts as a pro-oxidant in a cell culture model of diabetes-induced peripheral neuropathy. Redox Biology, 21, 101078. 10.1016/j.redox.2018.101078 [PubMed: 30593978]

Timme-Laragy AR, Goldstone JV, Imhoff BR, Stegeman JJ, Hahn ME, & Hansen JM (2013). Glutathione redox dynamics and expression of glutathione-related genes in the developing embryo. Free Radical Biology and Medicine, 65, 89–101. 10.1016/j.freeradbiomed.2013.06.011 [PubMed: 23770340]

Tonelli C, Chio IIC, & Tuveson DA (2018). Transcriptional Regulation by Nrf2. Antioxidants & Redox Signaling, 29(17), 1727–1745. 10.1089/ars.2017.7342 [PubMed: 28899199]

Tung EWY, & Winn LM (2011). Valproic Acid Increases Formation of Reactive Oxygen Species and Induces Apoptosis in Postimplantation Embryos: A Role for Oxidative Stress in Valproic Acid-Induced Neural Tube Defects. Molecular Pharmacology, 80(6), 979–987. 10.1124/mol.111.072314 [PubMed: 21868484]

Author Manuscript Author Manuscript Author Manuscript Author Manuscript

Vajda FJ, O'Brien TJ, Graham JE, Lander CM, & Eadie MJ (2013). Dose dependence of fetal malformations associated with valproate. Neurology, 81(11), 999–1003. 10.1212/WNL.0b013e3182a43e81 [PubMed: 23911758]

Venugopal R, & Jaiswal AK (1996). Nrf1 and Nrf2 positively and c-Fos and Fra1 negatively regulate the human antioxidant response element-mediated expression of NAD(P)H:quinone oxidoreductase1 gene. Proceedings of the National Academy of Sciences, 93(25), 14960–14965. 10.1073/pnas.93.25.14960

Wang L, Wang M, Hu J, Shen W, Hu J, Yao Y, Wang X, Afzal CM, Ma R, & Li G (2017). Protective effect of 3H-1, 2-dithiole-3-thione on cellular model of Alzheimer's disease involves Nrf2/ARE signaling pathway. European Journal of Pharmacology, 795, 115–123. 10.1016/j.ejphar.2016.12.013 [PubMed: 27939991]

Wild AC, Moinova HR, & Mulcahy RT (1999). Regulation of γ-Glutamylcysteine Synthetase Subunit Gene Expression by the Transcription Factor Nrf2. Journal of Biological Chemistry, 274(47), 33627–33636. 10.1074/jbc.274.47.33627

Xiao H, Jedrychowski MP, Schweppe DK, Huttlin EL, Yu Q, Heppner DE, Li J, Long J, Mills EL, Szpyt J, He Z, Du G, Garrity R, Reddy A, Vaites LP, Paulo JA, Zhang T, Gray NS, Gygi SP, & Chouchani ET (2020). A Quantitative Tissue-Specific Landscape of Protein Redox Regulation during Aging. Cell, 180(5), 968–983.e24. 10.1016/j.cell.2020.02.012 [PubMed: 32109415]

Author Manuscript Author Manuscript Author Manuscript Author Manuscript

Highlights

- Total GSH, Cys and respective E_h fluctuate in control tissues and fluids on GD 8–9
- *In vitro* VPA exposure spatially and temporally alters GSH and Cys redox status
- VPA limits amino acid supply for GSH synthesis by attenuation of VYS protein uptake
- D3T activates Nrf2 protection systems but does not sustain elevated global GSH
- Combined VPA+D3T does not consistently prevent oxidation events caused by VPA alone

Author Manuscript Author Manuscript Author Manuscript Author Manuscript

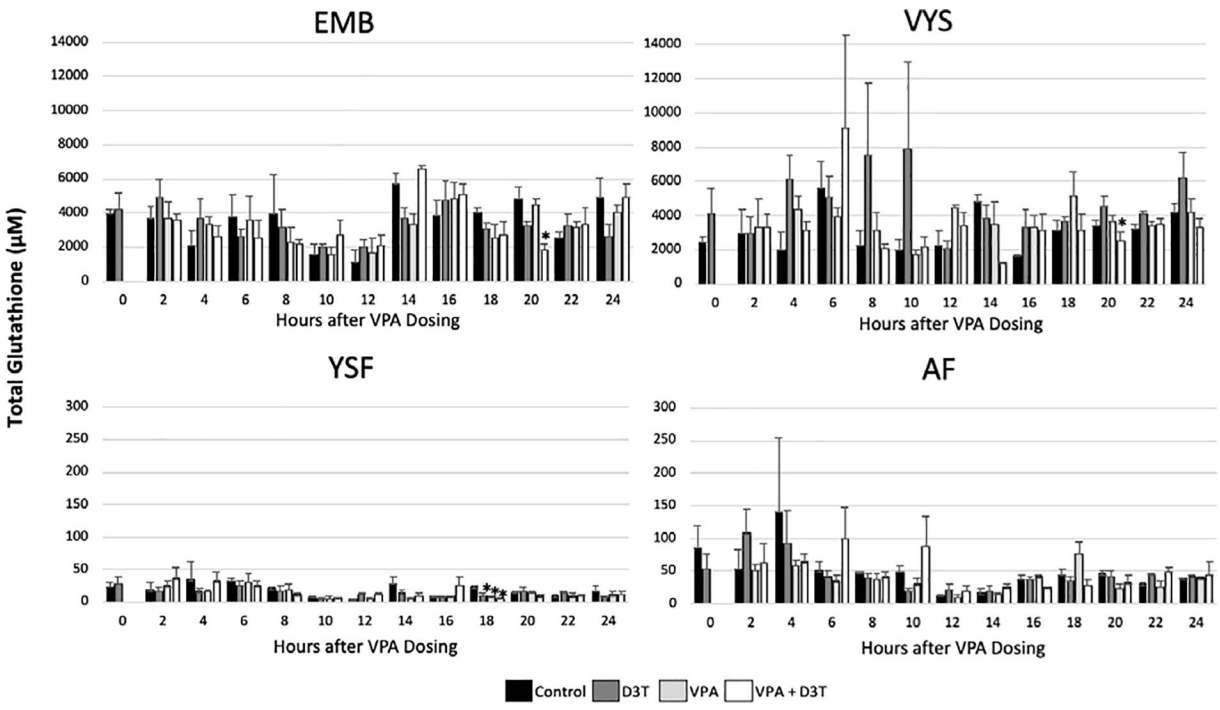

Figure 1:

Total Glutathione (GSH+2GSSG) concentration was measured by HPLC every 2 hours over 24 hours of mouse neurulation in the embryo (EMB), visceral yolk sac (VYS), yolk sac fluid (YSF), and amniotic fluid (AF) (n=3). D3T (10 µM) pre-treatment began 2 hours prior to dosing of VPA (600 µM) at 0 hours. All dosing was done directly in the culture medium. Error bars represent standard error. * $p<0.05$ compared to control within timepoint.

Author Manuscript Author Manuscript Author Manuscript Author Manuscript

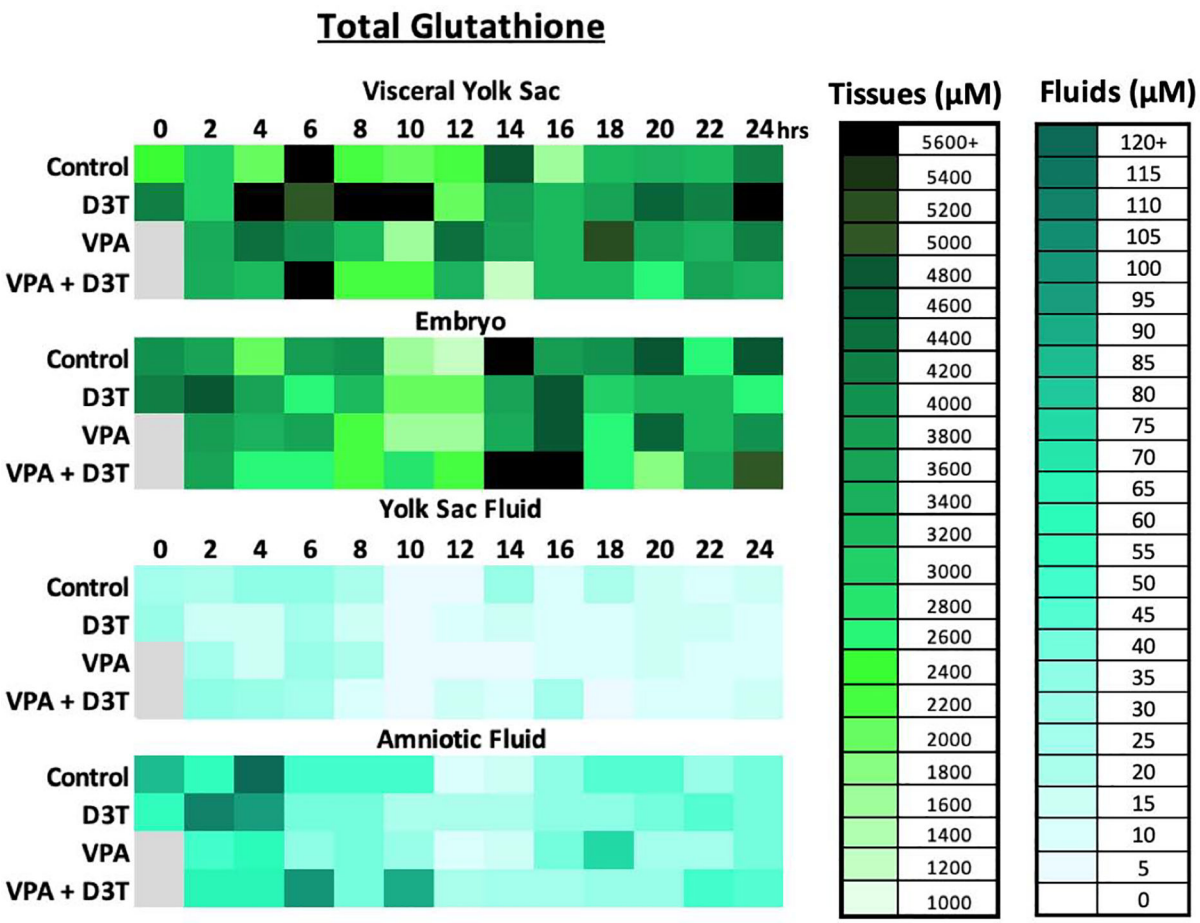

Figure 2:

Total Glutathione (GSH+2GSSG) concentration was measured by HPLC every 2 hours over 24 hours of mouse neurulation in the embryo (EMB), visceral yolk sac (VYS), yolk sac fluid (YSF), and amniotic fluid (AF) (n=3). D3T (10 µM) pre-treatment began 2 hours prior to dosing of VPA (600 µM) at 0 hours. All dosing was done directly in the culture medium.

Author Manuscript Author Manuscript Author Manuscript Author Manuscript

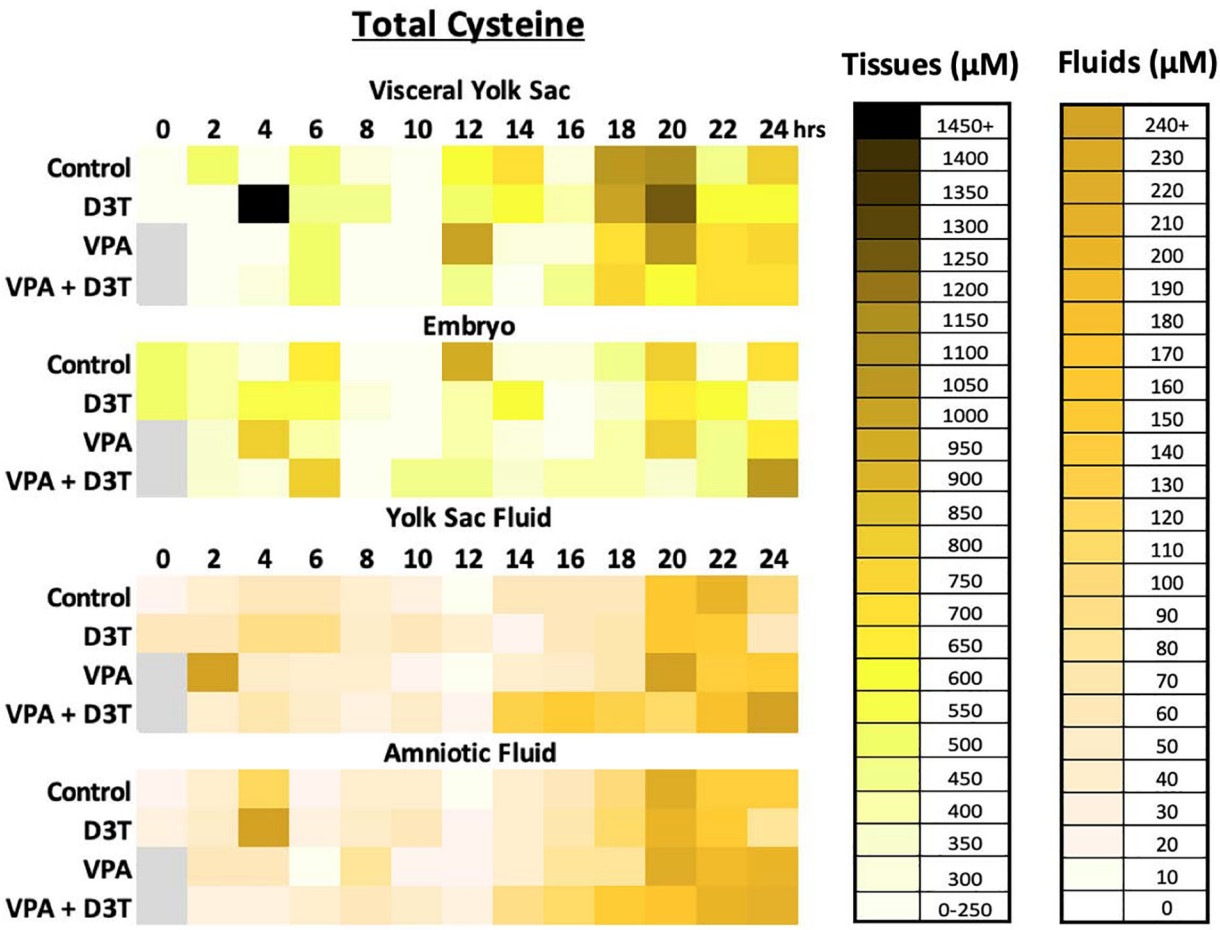

Figure 3:

Total Cysteine (Cys+2CySS) concentration was measured by HPLC every 2 hours over 24 hours of mouse neurulation in the embryo (EMB), visceral yolk sac (VYS), yolk sac fluid (YSF), and amniotic fluid (AF) (n=3). D3T (10 µM) pre-treatment began 2 hours prior to dosing of VPA (600 µM) at 0 hours. All dosing was done directly in the culture medium.

Author Manuscript Author Manuscript Author Manuscript Author Manuscript

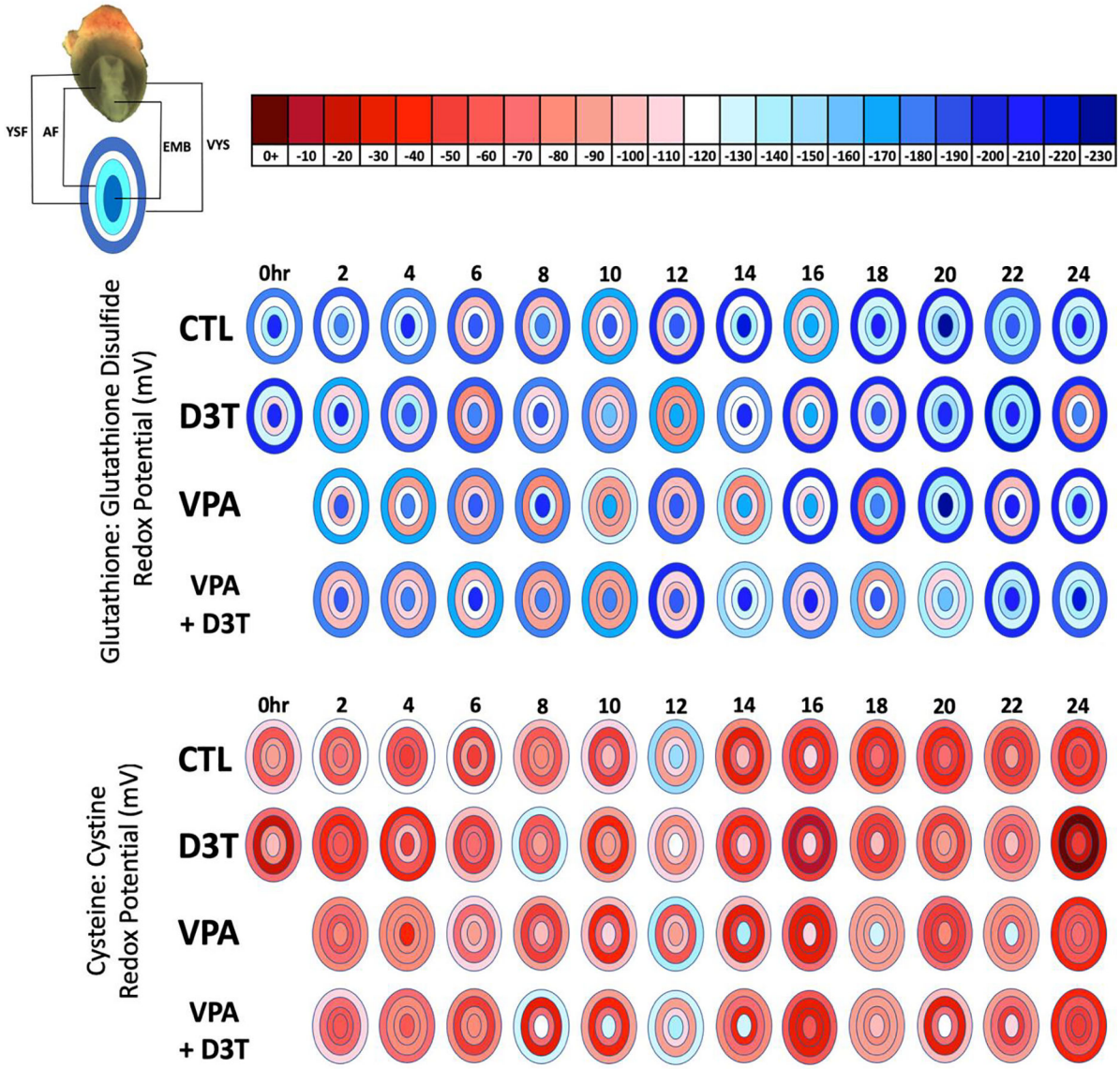

Figure 4:

GSSG and Cys:CySS redox potentials (E_h) were measured by HPLC every 2 hours across 24 hours of mouse neurulation in the embryo (EMB), visceral yolk sac (VYS), yolk sac fluid (YSF), and amniotic fluid (AF) (n=3). Redox Potential was calculated using the Nernst equation. Negative values are more reducing and positive values are more oxidizing. D3T (10 μM) pre-treatment began 2 hours prior to dosing of VPA (600 μM) at 0 hours. All dosing was directly in the culture medium of female rat serum.

Author Manuscript Author Manuscript Author Manuscript Author Manuscript

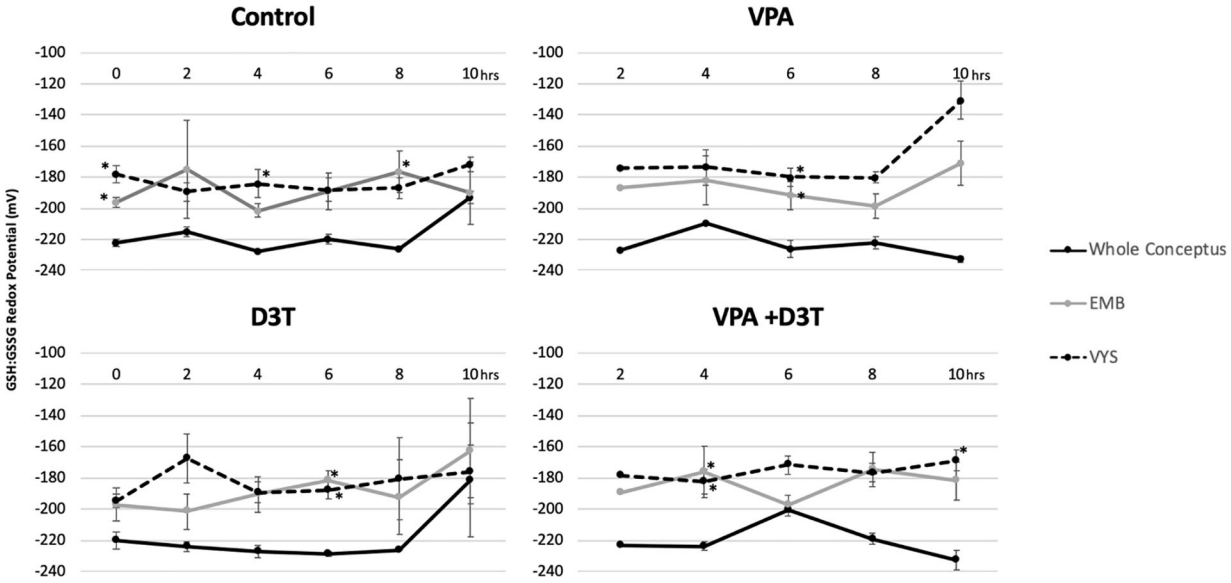

Figure 5:

Whole Conceptus (n=2) GSH:GSSG redox potential (E_h) compared to embryo (EMB) and visceral yolk sac (VYS) (n=3) redox potential after 0–10 hours of exposure in Control, D3T (10 μM), VPA (600 μM), and VPA +D3T (600 μM +10 μM) treatment groups. *p<0.05 compared to the whole conceptus value.

Author Manuscript Author Manuscript Author Manuscript Author Manuscript

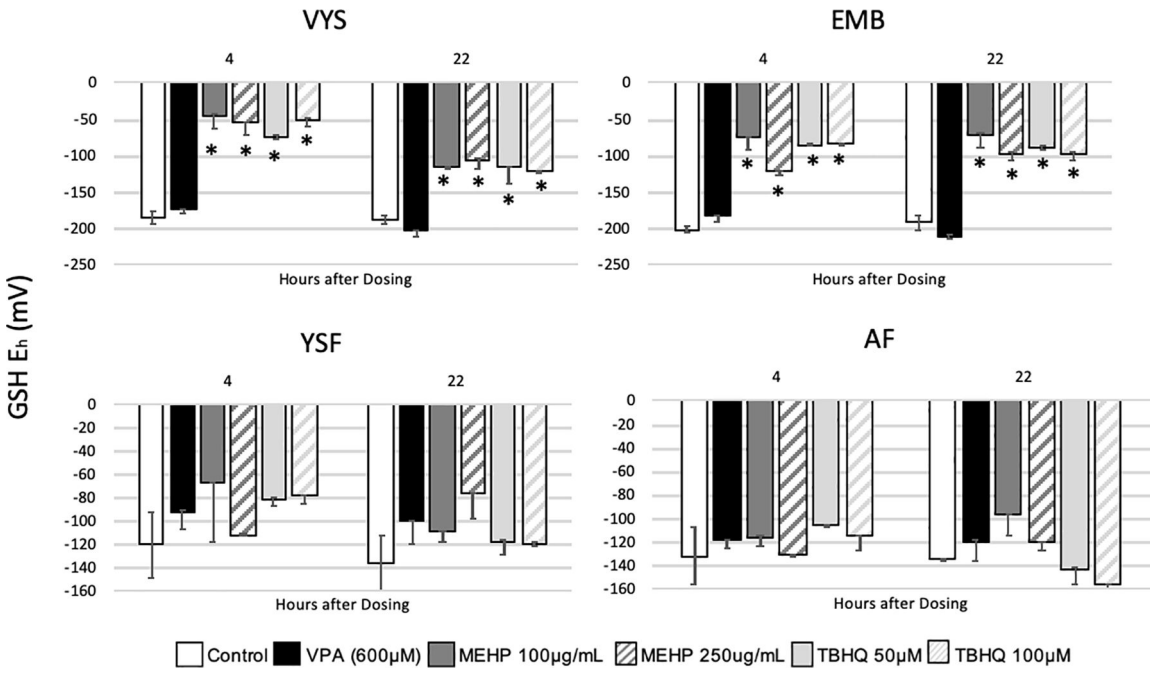

Figure 6:

GSH:GSSG redox potential (E_h) in VYS and EMB following dosing with VPA (600 μM, n=3), MEHP (100 and 250 μg/ml, n=2)or TBHQ (50 and 100 μM, n=2) for 4 and 22 hours. Error bars represent standard error. *p<0.05 compared to the control.

Author Manuscript Author Manuscript Author Manuscript Author Manuscript

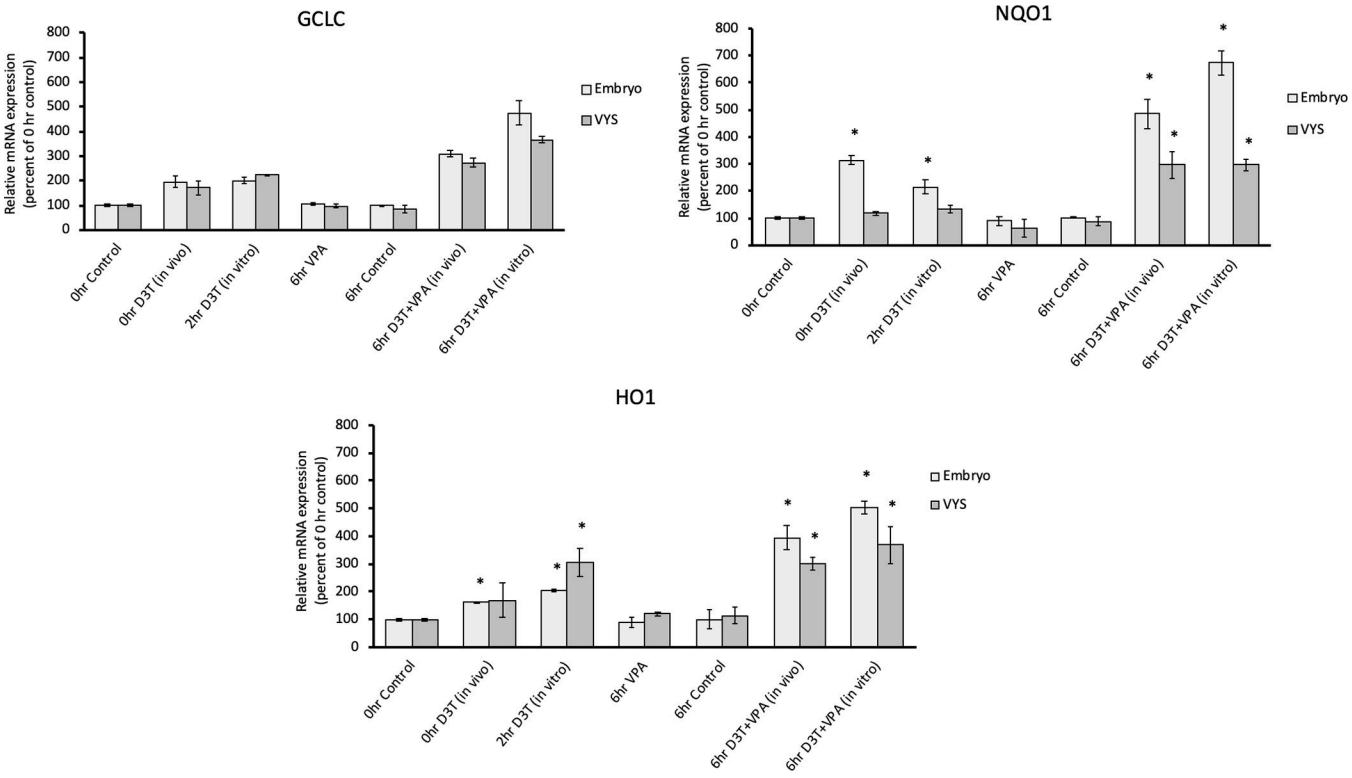

Figure 7:

RT-qPCR measurement of Nrf2 antioxidant pathway genes *GCLC, H01,* and *NQ01* in the EMB and VYS following treatment with *in vivo* D3T (5mg/kg), *in vitro* D3T (10 μM) or VPA (600 μM). Results are represented as fold-changes relative to the 0hr control with normalization based on housekeeping gene *B-actin*. n=3, *p<0.05

Author Manuscript Author Manuscript Author Manuscript Author Manuscript

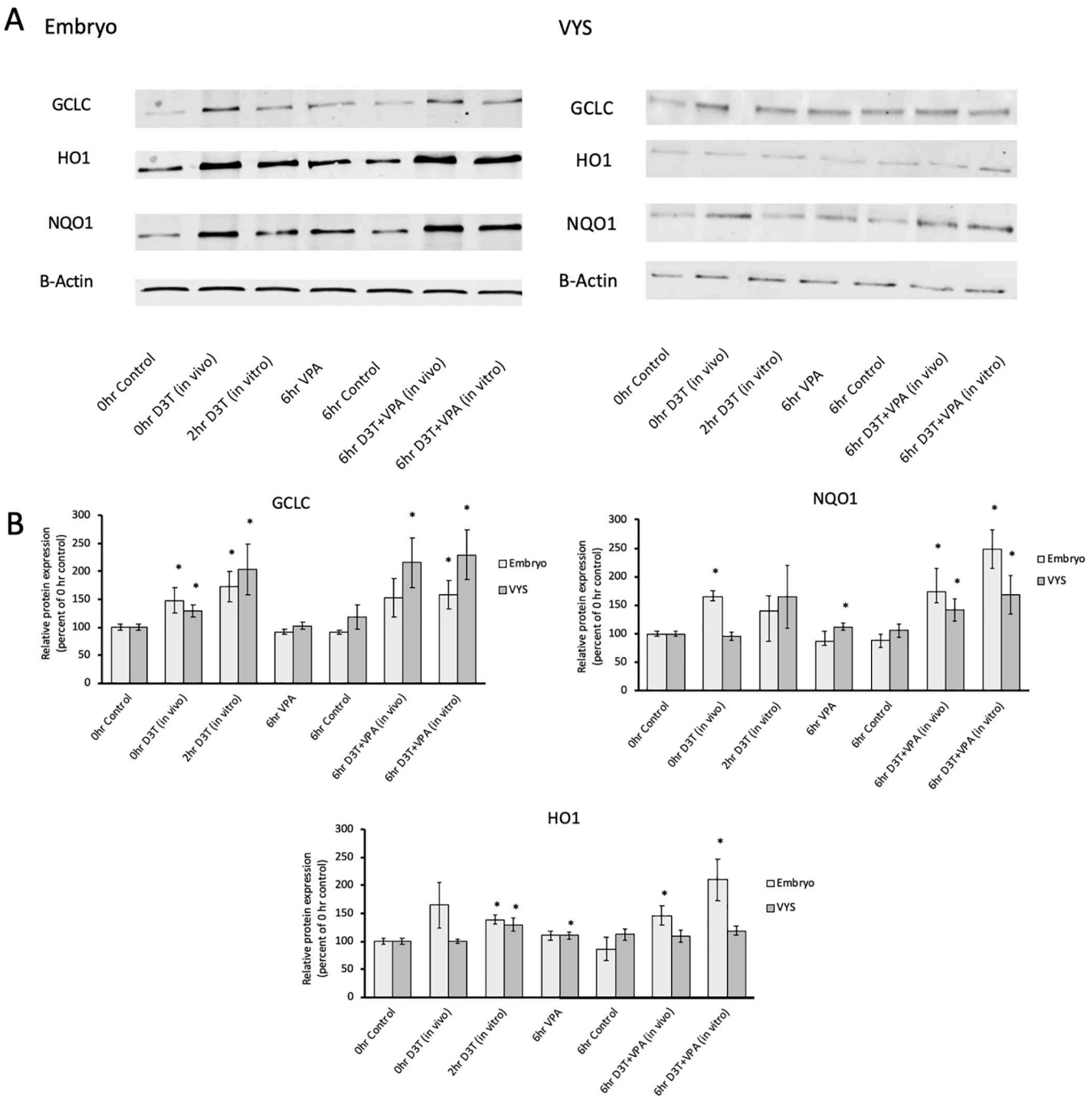

Figure 8:

Protein expression of Nrf2 antioxidant pathway genes *GCLC, H01,* and *NQ01* in the EMB and VYS following treatment with *in vivo* D3T (5mg/kg), *in vitro* D3T (10 μM) or VPA (600 μM). A: Western Blot Images B: Results are represented as fold-changes relative to the 0hr control with normalization based on housekeeping gene *B-actin*. n=3, *p<0.05

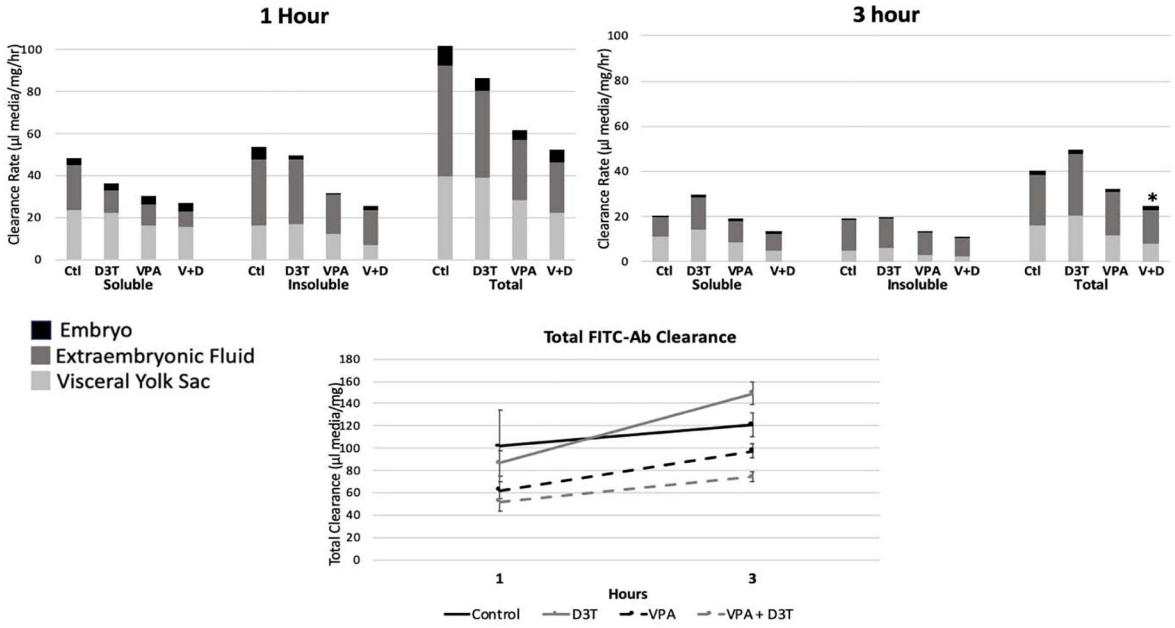

Figure 9:

Histiotrophic nutrition evaluated at 1 and 3 hours through FITC-Ab clearance. Total clearance is the sum of FITC-Ab fluorescence across VYS, EMB, and EEF. Acid insoluble and soluble fluorescence represent intact and degraded proteins respectively. n=6, *p<0.05 compared to the control. Error bars for total clearance represent standard error.

Author Manuscript Author Manuscript Author Manuscript Author Manuscript